

Emergence Of Directional Rotation In Optothermally Activated Colloidal System

Rahul Chand,^{†,¶} Chaudhary Eksha Rani,^{†,¶} Diptabrata Paul,^{†,‡} and G V Pavan
Kumar^{*,†}

[†]*Department of Physics, Indian Institute of Science Education and Research (IISER),
Pune 411008, India*

[‡]*Present address: Faculty for Physics and Earth Sciences, Leipzig University*

[¶]*These authors contributed equally to this work*

E-mail: pavan@iiserpune.ac.in

Abstract

We experimentally demonstrate the emergence of directional rotation in thermally active-passive colloidal structures under optical confinement. The observed handedness of rotation of the structure can be controlled by changing the relative position of the constituent colloids. We show that the angular velocity of rotation is sensitive to the intensity of the incident optical fields and the size of the constituent colloidal entities. The emergence of rotational dynamics can be understood in the context of asymmetric temperature distribution in the system and the relative location of the active colloid, which creates a local imbalance of optothermal torques to the confined system. Our work demonstrates how localized optothermal fields lead to directional rotational dynamics without explicitly utilizing spin or orbital angular momentum of light. We envisage that our results will have implications in realizing Brownian engines, and can directly relate to rotational dynamics in biological and ecological systems.

Introduction

Systems which are out-of-equilibrium are ubiquitous in nature¹⁻⁷. These systems exhibit interesting emergent dynamics such as dynamic self-assembly,⁸⁻¹⁰ pattern formation¹¹⁻¹⁴ and collective motility (both in terms of translation and rotation).^{1,6,15-20} These phenomena emerge due to the mutual interaction between the individual elements of these collective systems. Understanding the underlying principle behind these collective phenomena motivates researchers to emulate similar behavior in laboratory environments, which is one of the key goals of active matter research²¹⁻²⁵. In this regard, artificial soft matter systems such as synthetic colloids can be used as test beds. Using such systems, we can study the interaction between individual entities that lead to collective behaviour, and understand the role of environmental cues that drive such systems.

In this context, two interrelated tasks have been pursued: first, a variety of colloidal matter has been realized and studied in the context of active systems²⁶⁻³¹. Second, diverse methods including chemical³²⁻³⁵, electric³⁶⁻³⁸, magnetic,³⁹⁻⁴⁴ and optical fields⁴⁵⁻⁵⁶ have been innovated that can act as an environmental cue to translate and rotate soft systems.

The point of interest to the current study is the rotational dynamics. The emergence of rotational degrees of freedom has been observed in a variety of natural systems,^{10,15,16,19,57-59} and emulating them using artificial soft matter systems^{26,60-62} is an interesting but challenging task.

Among the available tools, optical fields have emerged as versatile and complementary methods to not only drive soft systems but also confine them⁶³⁻⁶⁶. In the context of generating rotational degrees of freedom, the spin and the orbital angular momentum of light⁶⁷⁻⁷³ has been extensively utilized. A relevant question to ask is: can we introduce rotational degrees of freedom in an active colloidal system without using the spin or orbital angular momenta of light? This will create new and complementary opportunities to manipulate soft systems without having to depend on the angular momentum of light.

One of the ways to do so is to utilize optothermal effects⁷⁴, where localized optical heating

can create asymmetric temperature gradients, thereby breaking the symmetry that results in rotation^{60–62,75–77}. To gain control over this approach, there is now an imperative to identify the material parameters of thermally active colloids and the nature of optothermal fields that generate rotation. Specifically, generating directional rotation in the artificial active matter has emerged as an important task^{30,35,75}, which needs attention for both fundamental understanding and biological and technological applications.

Motivated by this, here we present our experimental observation of generating directional rotation in colloidal structures composed of thermally active (A) and passive (P) colloids under 532 nm laser beam illumination. Figure 1(a) shows a typical schematic of rotation in a trimer structure where P1, P2, and A are the passive and thermally active colloids respectively. Here the passive colloids P1 and P2 are almost identical, the only difference between them is their position with respect to the laser beam center. The handedness of this rotational motion depends on the relative position of the colloid A in the structure, which is evident from Figure 1(b) and Figure 1(c). Furthermore, we have shown how such rotation can be controlled by using a combination of colloids and the intensity of optical fields. We will first discuss the experimental methods used in the realization of such dynamics followed by a detailed discussion of the directional rotation.

Results and discussion

In our experiments, we have used two types of colloids (i) passive colloids denoted by P and (ii) thermally active colloids denoted by A. Melamine formaldehyde (MF) (diameter 2.0 μm) and polystyrene (PS) particles (diameter 1.3 μm) have been used as passive colloids and iron oxide doped polystyrene (PS) particles (diameter 1.3 μm) have been used as thermally active colloids (obtained from Microparticles GmbH). The iron-oxide nanoparticles in the thermally active colloids lead to the absorption of incident optical field and the consequent generation of thermal fields⁷⁸ (Supporting Information S1). These thermally active and passive colloids

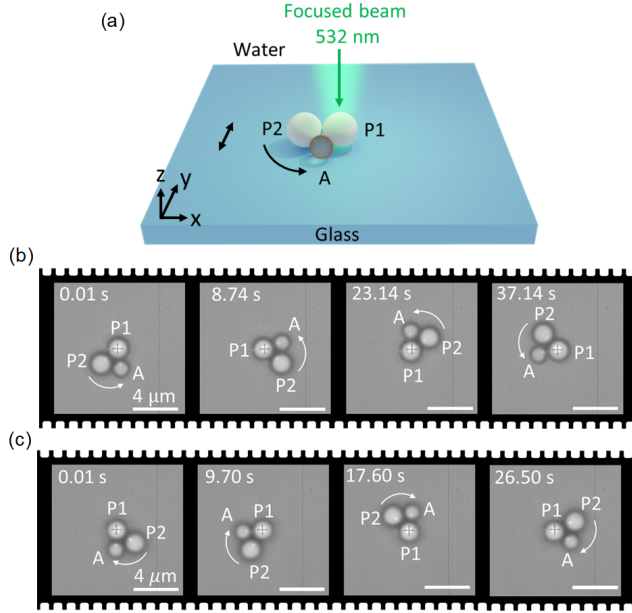


Figure 1: Rotation of a trimer structure in an optical field. (a) Schematic of the experiment. In a focused linearly polarized Gaussian laser beam of wavelength 532 nm, a trimer structure with two passive melamine formaldehyde colloids (P1 and P2) of diameter 2.0 μm and one thermally active polystyrene colloid (A) with diameter 1.3 μm exhibits rotation. The beam is polarized along the y -axis as indicated by the double-sided black arrow. The direction of rotation is indicated by a curved black arrow. In (b) and (c) time series of rotation of two trimer structures with different handedness have been shown at 5.7 $\text{mW}/\mu\text{m}^2$ laser intensity. The position of the beam center is indicated by the grey ‘+’ symbol.

are dispersed in an aqueous suspension. 10 μL of the sample solution is dropcasted onto a chamber of height $\simeq 100 \mu\text{m}$, enclosed between two glass coverslips. The sample cell is then placed in a dual-channel optical microscopy setup as shown in Supporting Information S2. A linearly polarized Gaussian laser beam of wavelength 532 nm is focused on the lower coverslip using a 100×0.95 NA objective lens. The signal is then collected through a 100×1.49 NA oil immersion objective lens and projected to a fast camera to record the dynamics of colloids at 100 fps. The experimental laser beam profile is shown in Supporting Information S3. The trajectory of individual colloids are extracted from the recorded videos.⁷⁹

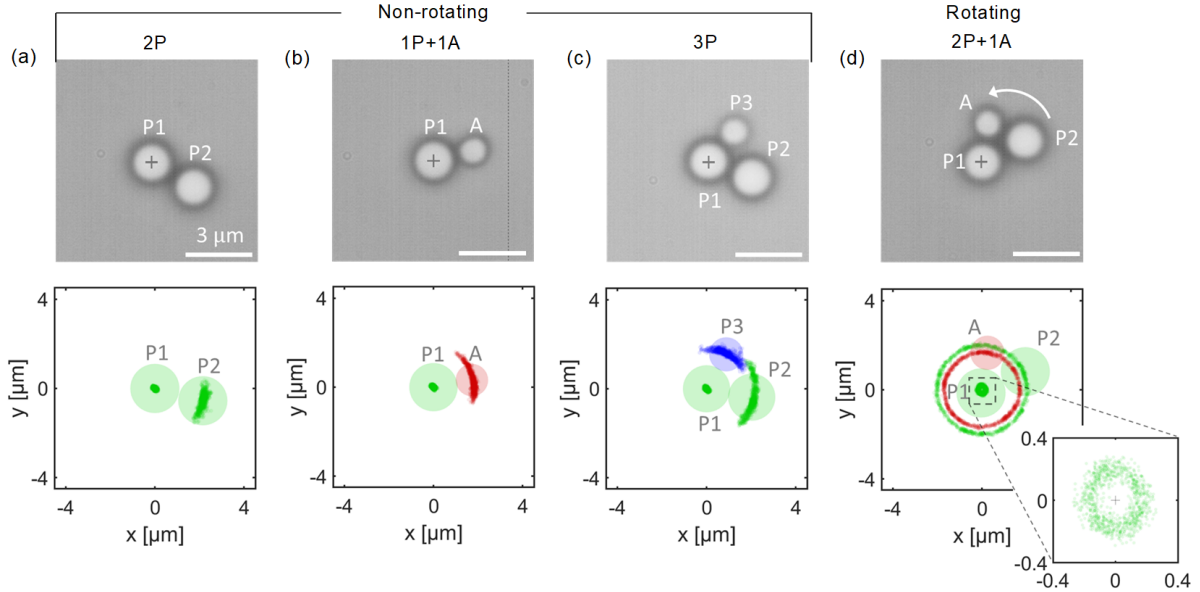


Figure 2: Dynamics of structures composed of passive and thermally active colloids at $5.7 \text{ mW}/\mu\text{m}^2$ laser intensity. No rotational motion is observed in dimer structures composed of (a) two passive MF colloids (P1, P2) and (b) one passive MF colloid (P1) and one thermally active PS colloid (A). (c) Passive trimer structure composed of two passive MF colloids (P1, P2) and one passive PS colloid (P3) does not exhibit any rotational dynamics. (d) Active trimer composed of two passive MF colloids (P1, P2) and one thermally active PS colloid (A) exhibits counterclockwise rotation. Inset shows the magnified position distribution of the central passive colloid (P1) which is directly trapped at beam center. Here the diameters of the colloids are $d_{P1} = d_{P2} = 2.0 \mu\text{m}$ and $d_{P3} = d_A = 1.3 \mu\text{m}$ and all the position distributions are taken over 50 seconds.

Dynamics of colloidal structures under optothermal confinement

To understand the colloidal configuration leading to the emergence of rotation, we have systematically studied four different structures under optical confinement as shown in Figure 2(a)-2(d). The structures are composed of (a) two passive colloids (P1, P2), (b) one passive (P1) and one thermally active colloid (A), (c) three passive colloids (P1, P2, P3), and (d) two passive (P1, P2) and one thermally active colloid (A) respectively. Out of these four structures, only the structure shown in Figure 2(d) exhibits rotational motion. The colloids in the dimer structures, in Figure 2(a) and Figure 2(b), are confined radially to the beam center as a result of optical gradient forces and do not exhibit any rotational motion. If one more passive polystyrene colloid (P3) of diameter $d_{P3} = 1.3 \mu\text{m}$ is added to the structure shown in

Figure 2(a), a trimer structure is formed (Figure 2(c)), aided by the optical gradient force-induced radial confinement. The non-rotating nature signifies the passivity of the system and therefore we indicate this as a passive trimer (PT) structure. But, when P3, in Figure 2(c), is replaced by a thermally active PS colloid (A) of the same size, rotational motion is observed as shown in Figure 2(d), thereby rendering an active trimer (AT) structure (see SI video 1). The position distribution of P1, shown in the inset, indicates the rotation of the whole structure about a common center. The angular velocity of such a rotating structure is obtained by calculating the differential cross-correlation function from the trajectory (x, y) of individual colloids as

$$\begin{aligned} dccf(\delta t) &= \frac{\langle x(t)y(t + \delta t) \rangle - \langle y(t)x(t + \delta t) \rangle}{\sqrt{\langle x^2(t) \rangle \langle y^2(t) \rangle}}, \\ &= Ae^{-\frac{\delta t}{\delta t_{ot}}} \sin(\omega \delta t), \end{aligned} \quad (1)$$

where δt , ω and δt_{ot} are lagtime, the angular velocity of rotation, and the characteristic timescale of the trap respectively⁶⁰. The angular velocity of rotation for AT, shown in Figure 2(d), is obtained as $\omega = 0.60$ rad/s. The magnitude of torque experienced by the system of colloids during this process can be estimated considering the moment of inertia I_i of corresponding colloids about the center of rotation (Supporting Information S4) as

$$|\tau| = \sum_i \frac{\gamma_i}{m_i} I_i \omega_i, \quad (2)$$

where ‘ i ’ represents individual colloids and γ_i (Supporting Information S5) and m_i are the friction coefficient and mass of the individual colloids respectively. The torque estimated for AT, shown in Figure 2(d), is $|\tau| \simeq 1.7 \cdot 10^{-19}$ Nm. Although both the trimer structures in Figure 2(c) and Figure 2(d) have almost similar compositions, only AT in Figure 2(d) exhibits rotational motion. Thus, the presence of thermally active colloid and the resultant generation of optothermal fields plays a crucial role in the rotation of the structure.

Optothermal forces and handedness of rotation of trimer structures

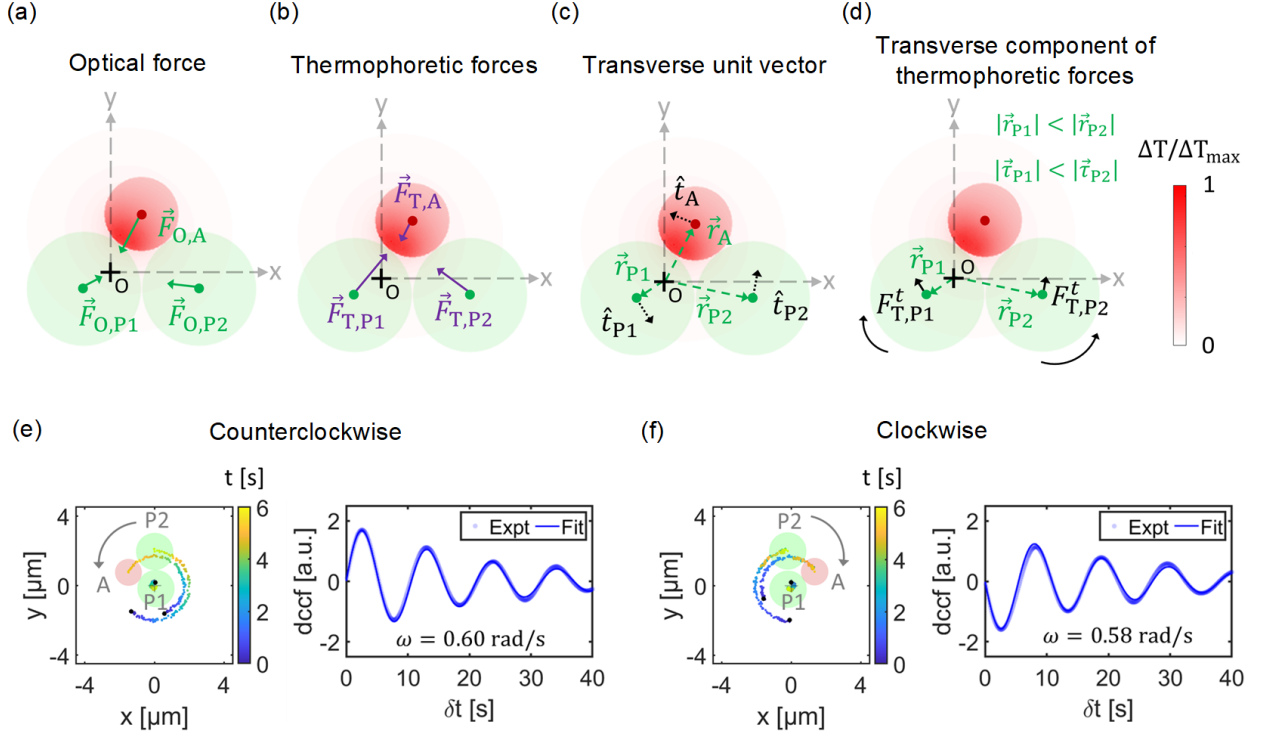


Figure 3: Optothermal forces and rotation of AT. Schematic force vector diagram of (a) optical gradient forces and (b) thermophoretic forces in AT structure, where '+' indicates the beam center. (c) Transverse unit vector at the location of individual colloids in the AT structure. (d) Transverse component of thermophoretic forces on P1 and P2. In (e) and (f) schematic trajectories of two AT structures exhibiting counterclockwise and clockwise rotation along with their calculated ddcfs are shown. The corresponding angular velocity of rotation at laser intensity = $5.7 \text{ mW}/\mu\text{m}^2$ is obtained as $\omega = 0.60 \text{ rad/s}$ and $\omega = 0.58 \text{ rad/s}$ respectively.

To understand the origin of rotation, we have qualitatively investigated different forces acting on the constituent colloids forming AT (shown in Figure 2(d)). The schematic vector diagram of different forces acting in an AT structure are shown in Figure 3(a) and 3(b). In the absence of peripheral colloids, P2 and A, the optical gradient force confines P1 to the beam center. But in the presence of the peripheral colloids, the optical gradient forces on P2 and A ($\vec{F}_{O,P2}$ and $\vec{F}_{O,A}$, indicated by green arrows in Figure 3(a)), lead to off-centered confinement of P1. Since the optical gradient forces, $\vec{F}_{O,i}$ on colloid i ($i = P1, P2$ and A) with position vector \vec{r}_i (measured from beam center O), are directed towards the beam center i.e. $\vec{F}_{O,i} \parallel \vec{r}_i$,

it implies they cannot induce rotation as $\vec{\tau} = \sum_i \vec{r}_i \times \vec{F}_{O,i} = 0$. This is evident from the absence of rotational motion in PT. Collectively $\vec{F}_{O,i}$ tends to confine the colloids to the beam center and the optical gradient force on P1 can be estimated as $F_{O, P1} = k(I_0) \cdot r_c \simeq 0.36$ pN, where r_c and $k(I_0)$ are the radius of rotation and the trap stiffness of P1 at laser intensity I_0 (Supporting Information S6). In addition, due to the thermophoretic behaviour of constituent colloids⁸⁰⁻⁸², the thermal field produced by colloid A exerts thermophoretic forces $\vec{F}_{T,i}$ on them, indicated by violet arrows in Figure 3(b). These $\vec{F}_{T,i}$ act from the particle center towards the positive temperature gradient and are not necessarily along radial direction. In our experimental configuration, the offset position of colloid A leads to an asymmetric temperature field around it. The side of colloid A close to the beam center has a higher temperature than the other sides (Supporting Information S7). This asymmetric temperature profile leads to different magnitudes of thermophoretic forces on P1 and P2 ($\vec{F}_{T, P1}$ and $\vec{F}_{T, P2}$). Besides, this asymmetric thermal field also leads to a self-thermophoretic force $\vec{F}_{T, A}$ on colloid A⁸³, due to thermo-osmotic fluid flow around it. However the exact experimental estimation of this asymmetric thermal field and thermophoretic forces are very difficult. For simplicity, we have considered that colloid A, which is at δx distance from the beam center, has a uniform surface temperature given by (see Supporting Information S7),

$$\Delta T(\delta x) = \Delta T_0(I_0) e^{-\frac{\delta x^2}{w_0^2}}, \quad (3)$$

where w_0 and $\Delta T_0(I_0)$ represent the beam waist and the maximum surface temperature of a centrally heated colloid A at laser intensity I_0 respectively. $\Delta T_0(I_0)$ is estimated using the nematic to isotropic phase transition of 5CB liquid crystals (Supporting Information S7). The approximation of uniform surface temperature of colloid A has been considered to get an approximate quantitative measure of its maximum surface temperature and the resulting thermophoretic forces and torques in such a structure. Under this approximation, the magnitude of the thermophoretic forces on P1 and P2 (which also have the contribution

from slip flow) are estimated as⁸⁴, $F_{T, P1} \simeq F_{T, P2} \simeq -\gamma D_T \nabla T \simeq 0.04$ pN, where D_T is the thermo-diffusion constant of P1 and P2 (Supporting Information S8). These $F_{T, P1}$ and $F_{T, P2}$ are acting along the colloid A (Supporting Information S9). Here the self-thermophoretic force on colloid A has not been taken care of because of the consideration of uniform surface temperature. These thermophoretic forces on colloid i ($i = P1, P2$) can be decomposed into radial ($F_{T,i}^r$) and transverse components ($F_{T,i}^t$) as $F_{T,i}^r = \vec{F}_{T,i} \cdot \hat{r}_i$ and $F_{T,i}^t = \vec{F}_{T,i} \cdot \hat{t}_i$, where \hat{r}_i and \hat{t}_i are the unit vectors along radial and the transverse direction respectively (see Figure 3(c)). Only the transverse components of these thermophoretic forces ($F_{T,i}^t$, indicated by black arrows in Figure 3(d)) give rise to the torque for rotation as, $\vec{\tau} = \sum_i \vec{r}_i \times \vec{F}_{T,i} = \sum_i r_i \cdot F_{T,i}^t$, where $i = P1$ and $P2$. In this way, we have obtained $F_{T, P1}^t \simeq -0.02$ pN and $F_{T, P2}^t \simeq 0.03$ pN. The negative $F_{T, P1}^t$ and positive $F_{T, P2}^t$ is because $F_{T, P1}^t$ on P1 is antiparallel to the transverse unit vector \hat{t}_{P1} at the position of P1, whereas $F_{T, P2}^t$ on P2 is parallel to the transverse unit vector \hat{t}_{P2} at the position of P2. While the torque ($\tau_{P1} \simeq -0.03 \cdot 10^{-19}$ Nm) induced by $F_{T, P1}^t$ on P1 tends to rotate the structure in a clockwise direction, the torque ($\tau_{P2} \simeq 0.62 \cdot 10^{-19}$ Nm) induced by $F_{T, P2}^t$ on P2 tends to rotate the structure in a counterclockwise direction. Although the magnitude of these transverse force components $F_{T, P1}^t$ and $F_{T, P2}^t$ are almost the same, due to the significant difference in the length of the force arm ($r_{P2} > r_{P1}$), the torques induced by them are significantly different in magnitude ($\tau_{P2} > \tau_{P1}$), resulting in a net torque which rotates the structure in a counterclockwise direction. Besides the rotation, it can also be noted that due to thermophoretic forces and slip flow-induced drag forces, the colloids in AT are much more tightly bound to each other than colloids in PT (Supporting Information S10).

Evidently, the rotation in AT is driven by the optothermal interaction facilitated between the constituent colloidal entities due to the asymmetric positioning of colloid A. Thus, by changing the relative position of colloid A in the AT, the sense of rotation can be controlled as shown in SI video 2. Figure 3(e) shows that if colloid A is positioned to the left of P2, then the AT will rotate counterclockwise. Whereas, if colloid A is positioned to the right side of

P2, the AT rotates in a clockwise direction as shown in Figure 3(f). We can even dynamically change the direction of rotation by switching the laser beam spot from one passive colloid to another (see SI video 3). The angular velocity of rotation (ω) of the AT structures (in Figure 3(e) and 3(f)) were obtained by calculating the dcf as, $\omega = 0.60$ rad/s and $\omega = 0.58$ rad/s respectively. The magnitude of the angular velocity of rotation (ω) is similar in both these cases but it may vary slightly among different ATs' because of non-uniform doping and size of constituent colloids.

To get further insight into the emergence of rotation in AT, we have simulated thermo-osmotic fluid flow around the structure by employing a finite element method-based numerical simulation technique (Supporting Information S11). The fluid-colloid interfaces are set to their respective thermo-osmotic slip coefficients (χ) estimated from their thermo-diffusion constant (D_T) as $\chi = 3/2TD_T$ (see Supporting Information S8). Additionally, colloid A is considered to serve as a heat source with uniform surface temperature governed by equation (3). The resultant thermo-osmotic slip flow velocity comes out to be $\simeq 1$ $\mu\text{m/s}$, leading to the approximate flow-induced drag force on P1 and P2 as 0.08 pN, which is comparable to the estimated thermophoretic forces (0.04 pN). The resultant slip flow-induced torque contribution is estimated as $\simeq 10^{-19}$ Nm which is of a similar order of magnitude as the experimental torque. The temperature-dependent density of the surrounding fluidic environment can also lead to convective fluid flow in the order of 1 nm/s, which can give rise to negligible torque contribution of $\simeq 10^{-24}$ Nm. Therefore, we can attribute the dominant contribution of torque to the thermo-osmotic flow field.

Control over the speed of rotation

While the sense of rotation of AT can be modulated by changing the orientation of constituent colloidal entities, the intensity of the incident laser beam can be used to control the corresponding angular velocity. Figure 4(a) shows that both the rotational speed as well as the torque produced in the AT increases almost linearly with increasing laser intensity. This

can be attributed to the linear increase in the average surface temperature of colloid A and corresponding thermophoretic forces with the intensity of the incident laser beam (Figure 4(b)). A similar linear incremental trend of the torque is also obtained from the simulation of the thermo-osmotic flow field (Supporting Information S11).

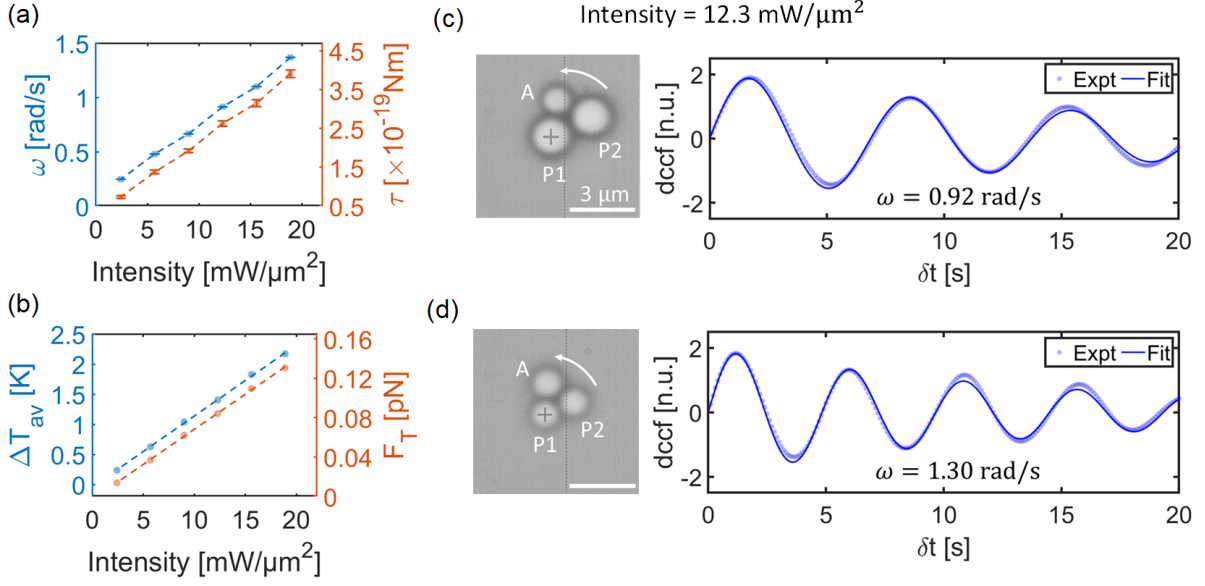


Figure 4: Control over rotational dynamics of AT. The rotational dynamics of AT structure depends on the laser intensity. (a) The estimated angular velocity of rotation (ω) and corresponding torque (τ) show an incremental trend with laser intensity. (b) Linear increment of the average surface temperature (ΔT_{av}) of the thermally active colloid (calculated from equation (3)) and thermophoretic force (F_T) with laser intensity. (c) and (d) show two AT structures, with diameter of P1 and P2 as $d_{P1} = d_{P2} = 2.0 \mu\text{m}$ and $d_{P1} = d_{P2} = 1.3 \mu\text{m}$ respectively along with their corresponding calculated dccf, where the diameter of colloid A is same $d_A = 1.3 \mu\text{m}$.

Besides the laser intensity, rotational dynamics of AT can also be modulated by changing the diameter of constituent passive colloids (P1, P2). This is because the thermal field, inertia, and friction coefficients of colloids in the structure get modified, as the diameter of passive colloids are changed. To see these effects, we have studied two AT structures having different sizes of passive colloids (see Figure 4(c) and 4(d)), where the diameter of P1 and P2 are $d_{P1} = d_{P2} = 2.0 \mu\text{m}$ and $d_{P1} = d_{P2} = 1.3 \mu\text{m}$ respectively (keeping diameter of colloid A same as $d_A = 1.3 \mu\text{m}$). The resulting torque imbalance induced by the thermophoretic forces ($F_T \simeq 0.08 \text{ pN}$ and 0.13 pN) are $\tau = 1.2 \cdot 10^{-19} \text{ Nm}$ and $1.45 \cdot 10^{-19} \text{ Nm}$ for structures shown

in Figure 4(c) and 4(d) respectively. Inserting the value of these torques into equation (2), we obtained that AT in Figure 4(c) should exhibit slower rotation ($\omega \simeq 0.43$ rad/s) than AT in Figure 4(d) ($\omega \simeq 1.2$ rad/s). This matches with the experimentally obtained trend of slower rotation ($\omega \simeq 0.92$ rad/s) for AT in Figure 4(c) than in Figure 4(d) ($\omega \simeq 1.30$ rad/s). In case of the bigger trimer, there is a significant deviation observed. This can be due to various reasons such as in our estimation, we have not considered the hydrodynamic interaction between the colloids.⁸⁵⁻⁸⁷ During the experimental estimation of the torque using the moment of inertia (I_i) of individual colloids, we used equation (2). Here the friction coefficient γ_i of individual colloids has been estimated from the free diffusion of colloids near a glass coverslip (Supporting Information S5), which can be significantly perturbed due to the presence of other colloids or surfaces nearby.^{88,89} If these considerations are taken into account, the theoretical and experimental values should converge.

Structures with a higher number of colloids

Since the induced thermal field plays a key role in the rotational dynamics, we can use additional thermally active colloids to modulate the rotational dynamics of the structures. Here, we explore the structure that emerges in such cases as well as their resultant dynamics (see SI video 4). The asymmetrical structures in Figure 5(a) and 5(b), have two thermally active colloids (A1, A2) on the same side of P2, exhibiting characteristic rotation. Since colloid A2 in Figure 5(a) is farther away from the beam center than in Figure 5(b), the effective surface temperature rise and consequently induced thermo-osmotic slip flow will be lesser for structure in Figure 5(a). As a result, the structure in Figure 5(a) exhibits slower rotation (0.39 rad/s) than that in Figure 5(b) (0.65 rad/s). In contrast, when colloids A1 and A2 are positioned on both sides of P2 as in Figure 5(c), then the thermophoretically induced torques due to colloid A1 and A2 will cancel each other resulting in the absence of rotational motion in the structure. The temporal evolution of such a structure, depicted in Supporting Information S12, shows rotational motion until the optothermal asymmetry and

hence thermophoretic force-induced torque imbalance is maintained.

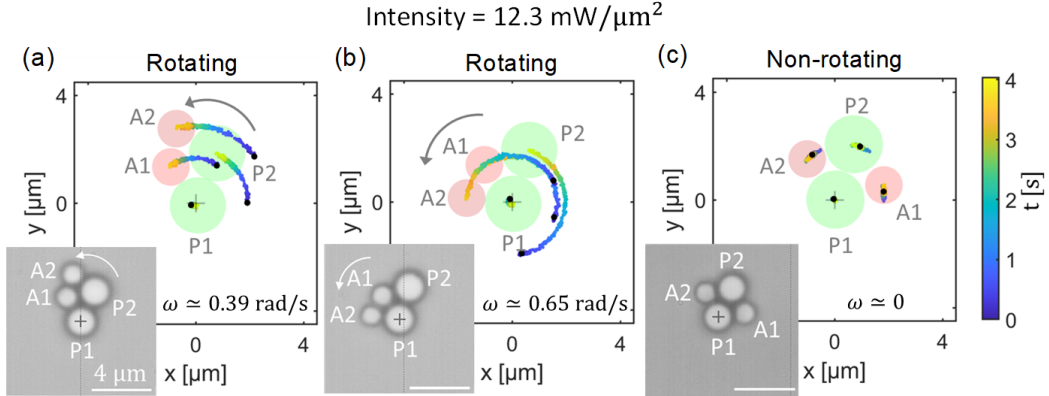


Figure 5: Rotational dynamics of structures composed of a higher number of colloids. (a)-(c) Show trajectories of differently oriented structures composed of two passive MF colloids (P1, P2) and two thermally active PS colloids (A1, A2) of diameters $d_{P1} = d_{P2} = 2 \mu\text{m}$ and $d_{A1} = d_{A2} = 1.3 \mu\text{m}$ respectively. Insets show bright field optical images. Structures shown in (a) and (b) exhibit rotational dynamics with an angular velocity of rotation of 0.39 rad/s and 0.65 rad/s respectively, whereas structure in (c) does not.

Conclusion

In conclusion, we have experimentally demonstrated the emergence of directional rotational motion of multi-component microscopic colloidal structures without any direct angular momentum transfer from optical fields. We have also shown that in our system we can dynamically control the handedness of rotation of the structure by changing its optothermal asymmetry. Our approach provides a clear advantage over fabricated asymmetric structures in view of dynamic control on the handedness of rotation^{60,61,90-93}. Further, we have also shown how the intensity of the incident optical field can be used as an environmental cue to modulate the rotational dynamics of optothermally assembled asymmetrical structures. Our approach of emulating rotational dynamics in thermally active-passive colloidal structures can be implemented in a wide variety of colloids in view of their thermophoretic nature. Similar directional rotations are also observed in natural out-of-equilibrium systems such as bacteria⁹⁴⁻⁹⁶ and sperm cells⁹⁷⁻⁹⁹. Thus, our approach can be a test bed for understanding

the dynamics of such out-of-equilibrium systems and the influence of environmental cues on their dynamics. Our findings can potentially be useful to study the interaction between collective self-propelling organism, and out-of-equilibrium thermodynamics at the microscale.

Acknowledgement

R.C. and C.E.R. thank Ashutosh Shukla and Sumant Panday for the fruitful discussion. G.V.P.K. also acknowledges Prof. Deepak Dhar from IISER Pune, Prof. Vijaykumar Krishnamurthy from I.C.T.S, Bengaluru, and Dr. Shradha Mishra from I.I.T.(BHU) for valuable discussion.

Funding sources

This work was partially funded by AOARD (grant number FA2386-22-1-4017) and Swarnajayanti fellowship grant (DST/SJF/PSA-02/2017-18).

Supporting Information Available

Supporting information containing the following information is available with the manuscript. S1: Scanning electron micrograph and ultraviolet-visible spectra of thermally active PS colloid, S2: Experimental setup, S3: Experimental laser beam profile, S4: Estimation of experimental torque, S5: Diffusion constant and friction coefficient of colloids, S6: Optical trapping of colloids, S7: Thermal field around thermally active PS colloid, S8: Thermodiffusion constant and thermo-osmotic slip coefficient of colloids, S9: Thermophoretic forces, S10: Interparticle distances in active and passive trimers, S11: Simulation of flow fields, S12: Temporal evolution of optothermally asymmetric structure.

Supporting videos: SI video 1: Dynamics of active-passive structures under focused illumination, SI video 2: Handedness of rotation of AT structures, SI video 3: Dynamic

change of direction of rotation, SI video 4: Dynamics of structures with more than three colloids.

To avail the supporting information and videos please click <https://drive.google.com/drive/folders/1Vnb735moAL8HBPDilJ5GIcjRwDUaEaX4?usp=sharing>.

References

- (1) Vicsek, T.; Zafeiris, A. Collective motion. *Physics reports* **2012**, *517*, 71–140.
- (2) Marchetti, M. C.; Joanny, J.-F.; Ramaswamy, S.; Liverpool, T. B.; Prost, J.; Rao, M.; Simha, R. A. Hydrodynamics of soft active matter. *Reviews of modern physics* **2013**, *85*, 1143.
- (3) Bernheim-Groswasser, A.; Gov, N. S.; Safran, S. A.; Tzlil, S. Living matter: mesoscopic active materials. *Advanced Materials* **2018**, *30*, 1707028.
- (4) Gnesotto, F. S.; Mura, F.; Gladrow, J.; Broedersz, C. P. Broken detailed balance and non-equilibrium dynamics in living systems: a review. *Reports on Progress in Physics* **2018**, *81*, 066601.
- (5) Aranson, I. S. Bacterial active matter. *Reports on Progress in Physics* **2022**, *85*, 076601.
- (6) Tan, T. H.; Mietke, A.; Li, J.; Chen, Y.; Higinbotham, H.; Foster, P. J.; Gokhale, S.; Dunkel, J.; Fakhri, N. Odd dynamics of living chiral crystals. *Nature* **2022**, *607*, 287–293.
- (7) Ji, F.; Wu, Y.; Pumera, M.; Zhang, L. Collective Behaviors of Active Matter Learning from Natural Taxes Across Scales. *Advanced Materials* **2023**, *35*, 2203959.
- (8) Whitesides, G. M.; Grzybowski, B. Self-assembly at all scales. *Science* **2002**, *295*, 2418–2421.

- (9) Copeland, M. F.; Weibel, D. B. Bacterial swarming: a model system for studying dynamic self-assembly. *Soft matter* **2009**, *5*, 1174–1187.
- (10) Vincenti, B.; Ramos, G.; Cordero, M. L.; Douarche, C.; Soto, R.; Clement, E. Magnetotactic bacteria in a droplet self-assemble into a rotary motor. *Nature communications* **2019**, *10*, 5082.
- (11) Budrene, E. O.; Berg, H. C. Dynamics of formation of symmetrical patterns by chemotactic bacteria. *Nature* **1995**, *376*, 49–53.
- (12) Tyson, R.; Lubkin, S.; Murray, J. D. A minimal mechanism for bacterial pattern formation. *Proceedings of the Royal Society of London. Series B: Biological Sciences* **1999**, *266*, 299–304.
- (13) Steager, E. B.; Kim, C.-B.; Kim, M. J. Dynamics of pattern formation in bacterial swarms. *Physics of Fluids* **2008**, *20*, 073601.
- (14) Curatolo, A.; Zhou, N.; Zhao, Y.; Liu, C.; Daerr, A.; Tailleur, J.; Huang, J. Cooperative pattern formation in multi-component bacterial systems through reciprocal motility regulation. *Nature Physics* **2020**, *16*, 1152–1157.
- (15) Czirók, A.; Ben-Jacob, E.; Cohen, I.; Vicsek, T. Formation of complex bacterial colonies via self-generated vortices. *Physical Review E* **1996**, *54*, 1791.
- (16) Ērglis, K.; Wen, Q.; Ose, V.; Zeltins, A.; Sharipo, A.; Janmey, P. A.; Cēbers, A. Dynamics of magnetotactic bacteria in a rotating magnetic field. *Biophysical journal* **2007**, *93*, 1402–1412.
- (17) Zhang, Y.; Ducret, A.; Shaevitz, J.; Mignot, T. From individual cell motility to collective behaviors: insights from a prokaryote, *Myxococcus xanthus*. *FEMS microbiology reviews* **2012**, *36*, 149–164.

- (18) Gachelin, J.; Rousselet, A.; Lindner, A.; Clement, E. Collective motion in an active suspension of *Escherichia coli* bacteria. *New Journal of Physics* **2014**, *16*, 025003.
- (19) Wioland, H.; Lushi, E.; Goldstein, R. E. Directed collective motion of bacteria under channel confinement. *New Journal of Physics* **2016**, *18*, 075002.
- (20) Meacock, O. J.; Doostmohammadi, A.; Foster, K. R.; Yeomans, J. M.; Durham, W. M. Bacteria solve the problem of crowding by moving slowly. *Nature Physics* **2021**, *17*, 205–210.
- (21) Sanchez, T.; Chen, D. T.; DeCamp, S. J.; Heymann, M.; Dogic, Z. Spontaneous motion in hierarchically assembled active matter. *Nature* **2012**, *491*, 431–434.
- (22) Takatori, S. C.; Brady, J. F. Towards a thermodynamics of active matter. *Physical Review E* **2015**, *91*, 032117.
- (23) Fodor, É.; Nardini, C.; Cates, M. E.; Tailleur, J.; Visco, P.; Van Wijland, F. How far from equilibrium is active matter? *Physical review letters* **2016**, *117*, 038103.
- (24) Jülicher, F.; Grill, S. W.; Salbreux, G. Hydrodynamic theory of active matter. *Reports on Progress in Physics* **2018**, *81*, 076601.
- (25) Shaebani, M. R.; Wysocki, A.; Winkler, R. G.; Gompper, G.; Rieger, H. Computational models for active matter. *Nature Reviews Physics* **2020**, *2*, 181–199.
- (26) Bricard, A.; Caussin, J.-B.; Das, D.; Savoie, C.; Chikkadi, V.; Shitara, K.; Chepizhko, O.; Peruani, F.; Saintillan, D.; Bartolo, D. Emergent vortices in populations of colloidal rollers. *Nature communications* **2015**, *6*, 7470.
- (27) Wang, W.; Duan, W.; Ahmed, S.; Sen, A.; Mallouk, T. E. From one to many: Dynamic assembly and collective behavior of self-propelled colloidal motors. *Accounts of chemical research* **2015**, *48*, 1938–1946.

- (28) Bechinger, C.; Di Leonardo, R.; Löwen, H.; Reichhardt, C.; Volpe, G.; Volpe, G. Active particles in complex and crowded environments. *Reviews of Modern Physics* **2016**, *88*, 045006.
- (29) Singh, D. P.; Choudhury, U.; Fischer, P.; Mark, A. G. Non-Equilibrium Assembly of Light-Activated Colloidal Mixtures. *Advanced Materials* **2017**, *29*, 1701328.
- (30) Schmidt, F.; Liebchen, B.; Löwen, H.; Volpe, G. Light-controlled assembly of active colloidal molecules. *The Journal of chemical physics* **2019**, *150*, 094905.
- (31) Wang, W.; Lv, X.; Moran, J. L.; Duan, S.; Zhou, C. A practical guide to active colloids: choosing synthetic model systems for soft matter physics research. *Soft Matter* **2020**, *16*, 3846–3868.
- (32) Kress, H.; Park, J.-G.; Mejean, C. O.; Forster, J. D.; Park, J.; Walse, S. S.; Zhang, Y.; Wu, D.; Weiner, O. D.; Fahmy, T. M.; others Cell stimulation with optically manipulated microsources. *Nature methods* **2009**, *6*, 905–909.
- (33) Soler, L.; Magdanz, V.; Fomin, V. M.; Sanchez, S.; Schmidt, O. G. Self-propelled micromotors for cleaning polluted water. *ACS nano* **2013**, *7*, 9611–9620.
- (34) Wang, H.; Zhao, G.; Pumera, M. Beyond platinum: bubble-propelled micromotors based on Ag and MnO₂ catalysts. *Journal of the American Chemical Society* **2014**, *136*, 2719–2722.
- (35) Wang, L.; Simmchen, J. Determination of the swimming mechanism of Au@ TiO₂ active matter and implications on active–passive interactions. *Soft Matter* **2023**, *19*, 540–549.
- (36) Velev, O. D.; Bhatt, K. H. On-chip micromanipulation and assembly of colloidal particles by electric fields. *Soft Matter* **2006**, *2*, 738–750.

- (37) Solodkov, N. V.; Saxena, A.; Jones, J. C. Electrically Driven Rotation and Nonreciprocal Motion of Microparticles in Nematic Liquid Crystals. *Small* **2020**, *16*, 2003352.
- (38) Senyuk, B.; Adufu, R. E.; Smalyukh, I. I. Electrically powered locomotion of dual-nature colloid-hedgehog and colloid-umbilic topological and elastic dipoles in liquid crystals. *Langmuir* **2022**, *38*, 689–697.
- (39) Tierno, P.; Golestanian, R.; Pagonabarraga, I.; Sagués, F. Controlled swimming in confined fluids of magnetically actuated colloidal rotors. *Physical review letters* **2008**, *101*, 218304.
- (40) Tierno, P.; Golestanian, R.; Pagonabarraga, I.; Sagués, F. Magnetically actuated colloidal microswimmers. *The Journal of Physical Chemistry B* **2008**, *112*, 16525–16528.
- (41) Tottori, S.; Zhang, L.; Qiu, F.; Krawczyk, K. K.; Franco-Obregón, A.; Nelson, B. J. Magnetic helical micromachines: fabrication, controlled swimming, and cargo transport. *Advanced materials* **2012**, *24*, 811–816.
- (42) Yu, H.; Tang, W.; Mu, G.; Wang, H.; Chang, X.; Dong, H.; Qi, L.; Zhang, G.; Li, T. Micro-/nanorobots propelled by oscillating magnetic fields. *Micromachines* **2018**, *9*, 540.
- (43) Zhou, H.; Mayorga-Martinez, C. C.; Pané, S.; Zhang, L.; Pumera, M. Magnetically driven micro and nanorobots. *Chemical Reviews* **2021**, *121*, 4999–5041.
- (44) Tierno, P.; Snezhko, A. Transport and assembly of magnetic surface rotors. *ChemNanoMat* **2021**, *7*, 881–893.
- (45) Ashkin, A.; Dziedzic, J. M.; Bjorkholm, J. E.; Chu, S. Observation of a single-beam gradient force optical trap for dielectric particles. *Optics letters* **1986**, *11*, 288–290.
- (46) Grier, D. G. A revolution in optical manipulation. *nature* **2003**, *424*, 810–816.

- (47) Dholakia, K.; Reece, P.; Gu, M. Optical micromanipulation. *Chemical Society Reviews* **2008**, *37*, 42–55.
- (48) Gao, D.; Ding, W.; Nieto-Vesperinas, M.; Ding, X.; Rahman, M.; Zhang, T.; Lim, C.; Qiu, C.-W. Optical manipulation from the microscale to the nanoscale: fundamentals, advances and prospects. *Light: Science & Applications* **2017**, *6*, e17039–e17039.
- (49) Polimeno, P.; Magazzu, A.; Iati, M. A.; Patti, F.; Saija, R.; Boschi, C. D. E.; Donato, M. G.; Gucciardi, P. G.; Jones, P. H.; Volpe, G.; others Optical tweezers and their applications. *Journal of Quantitative Spectroscopy and Radiative Transfer* **2018**, *218*, 131–150.
- (50) Shao, L.; Käll, M. Light-driven rotation of plasmonic nanomotors. *Advanced Functional Materials* **2018**, *28*, 1706272.
- (51) Šípová-Jungová, H.; Andrén, D.; Jones, S.; Käll, M. Nanoscale inorganic motors driven by light: Principles, realizations, and opportunities. *Chemical reviews* **2019**, *120*, 269–287.
- (52) Tkachenko, G.; Toftul, I.; Esporlas, C.; Maimaiti, A.; Le Kien, F.; Truong, V. G.; Chormaic, S. N. Light-induced rotation of dielectric microparticles around an optical nanofiber. *Optica* **2020**, *7*, 59–62.
- (53) Karpinski, P.; Jones, S.; Sipova-Jungova, H.; Verre, R.; Käll, M. Optical rotation and thermometry of laser tweezed silicon nanorods. *Nano Letters* **2020**, *20*, 6494–6501.
- (54) Bruce, G. D.; Rodríguez-Sevilla, P.; Dholakia, K. Initiating revolutions for optical manipulation: the origins and applications of rotational dynamics of trapped particles. *Advances in Physics: X* **2021**, *6*, 1838322.
- (55) Nan, F.; Li, X.; Zhang, S.; Ng, J.; Yan, Z. Creating stable trapping force and switchable optical torque with tunable phase of light. *Science Advances* **2022**, *8*, eadd6664.

- (56) Ding, H.; Chen, Z.; Kollipara, P. S.; Liu, Y.; Kim, Y.; Huang, S.; Zheng, Y. Programmable multimodal optothermal manipulation of synthetic particles and biological cells. *ACS nano* **2022**, *16*, 10878–10889.
- (57) Ishijima, S.; Hamaguchi, M. S.; Naruse, M.; Ishijima, S. A.; Hamaguchi, Y. Rotational movement of a spermatozoon around its long axis. *Journal of experimental biology* **1992**, *163*, 15–31.
- (58) Dominick, C. N.; Wu, X.-L. Rotating bacteria on solid surfaces without tethering. *Biophysical Journal* **2018**, *115*, 588–594.
- (59) Colin, R.; Drescher, K.; Sourjik, V. Chemotactic behaviour of *Escherichia coli* at high cell density. *Nature communications* **2019**, *10*, 5329.
- (60) Schmidt, F.; Magazzù, A.; Callegari, A.; Biancofiore, L.; Cichos, F.; Volpe, G. Microscopic engine powered by critical demixing. *Physical Review Letters* **2018**, *120*, 068004.
- (61) Peng, X.; Chen, Z.; Kollipara, P. S.; Liu, Y.; Fang, J.; Lin, L.; Zheng, Y. Opto-thermoelectric microswimmers. *Light: Science & Applications* **2020**, *9*, 141.
- (62) Bronte Ciriza, D.; Callegari, A.; Donato, M. G.; Çiçek, B.; Magazzù, A.; Kasianiuk, I.; Kasyanyuk, D.; Schmidt, F.; Foti, A.; Gucciardi, P. G.; others Optically Driven Janus Microengine with Full Orbital Motion Control. *ACS Photonics* **2023**, *10*, 3223–3232.
- (63) Spesyvtseva, S. E. S.; Dholakia, K. Trapping in a material world. *Acs Photonics* **2016**, *3*, 719–736.
- (64) Khadka, U.; Holubec, V.; Yang, H.; Cichos, F. Active particles bound by information flows. *Nature communications* **2018**, *9*, 3864.
- (65) Otte, E.; Denz, C. Optical trapping gets structure: Structured light for advanced optical manipulation. *Applied Physics Reviews* **2020**, *7*, 041308.

- (66) Volpe, G.; Maragò, O. M.; Rubinsztein-Dunlop, H.; Pesce, G.; Stilgoe, A. B.; Volpe, G.; Tkachenko, G.; Truong, V. G.; Chormaic, S. N.; Kalantarifard, F.; others Roadmap for optical tweezers. *Journal of Physics: Photonics* **2023**, *5*, 022501.
- (67) Volpe, G.; Petrov, D. Torque detection using Brownian fluctuations. *Physical review letters* **2006**, *97*, 210603.
- (68) Zhao, Y.; Shapiro, D.; Mcgloin, D.; Chiu, D. T.; Marchesini, S. Direct observation of the transfer of orbital angular momentum to metal particles from a focused circularly polarized Gaussian beam. *Optics express* **2009**, *17*, 23316–23322.
- (69) Donato, M.; Mazzulla, A.; Pagliusi, P.; Magazzù, A.; Hernandez, R.; Provenzano, C.; Gucciardi, P.; Maragò, O.; Cipparrone, G. Light-induced rotations of chiral birefringent microparticles in optical tweezers. *Scientific reports* **2016**, *6*, 31977.
- (70) Mazilu, M.; Arita, Y.; Vettenburg, T.; Auñón, J. M.; Wright, E. M.; Dholakia, K. Orbital-angular-momentum transfer to optically levitated microparticles in vacuum. *Physical Review A* **2016**, *94*, 053821.
- (71) Tamura, M.; Omatsu, T.; Tokonami, S.; Iida, T. Interparticle-interaction-mediated anomalous acceleration of nanoparticles under light-field with coupled orbital and spin angular momentum. *Nano Letters* **2019**, *19*, 4873–4878.
- (72) Tsuji, T.; Nakatsuka, R.; Nakajima, K.; Doi, K.; Kawano, S. Effect of hydrodynamic inter-particle interaction on the orbital motion of dielectric nanoparticles driven by an optical vortex. *Nanoscale* **2020**, *12*, 6673–6690.
- (73) Tao, Y.; Yokoyama, T.; Ishihara, H. Rotational dynamics of indirect optical bound particle assembly under a single tightly focused laser. *Optics Express* **2023**, *31*, 3804–3820.

- (74) Peterman, E. J.; Gittes, F.; Schmidt, C. F. Laser-induced heating in optical traps. *Biophysical journal* **2003**, *84*, 1308–1316.
- (75) Yang, M.; Ripoll, M. A self-propelled thermophoretic microgear. *Soft Matter* **2014**, *10*, 1006–1011.
- (76) Ding, H.; Chen, Z.; Ponce, C.; Zheng, Y. Optothermal rotation of micro-/nano-objects. *Chemical Communications* **2023**, *59*, 2208–2221.
- (77) Ding, H.; Kollipara, P. S.; Kim, Y.; Kotnala, A.; Li, J.; Chen, Z.; Zheng, Y. Universal optothermal micro/nanoscale rotors. *Science advances* **2022**, *8*, eabn8498.
- (78) Paul, D.; Chand, R.; Kumar, G. P. Optothermal Evolution of Active Colloidal Matter in a Defocused Laser Trap. *ACS Photonics* **2022**, *9*, 3440–3449.
- (79) Tinevez, J.-Y.; Perry, N.; Schindelin, J.; Hoopes, G. M.; Reynolds, G. D.; Laplantine, E.; Bednarek, S. Y.; Shorte, S. L.; Eliceiri, K. W. TrackMate: An open and extensible platform for single-particle tracking. *Methods* **2017**, *115*, 80–90.
- (80) Piazza, R.; Parola, A. Thermophoresis in colloidal suspensions. *Journal of Physics: Condensed Matter* **2008**, *20*, 153102.
- (81) Würger, A. Thermal non-equilibrium transport in colloids. *Reports on Progress in Physics* **2010**, *73*, 126601.
- (82) Liu, S.; Lin, L.; Sun, H.-B. Opto-thermophoretic manipulation. *Acs Nano* **2021**, *15*, 5925–5943.
- (83) Jiang, H.-R.; Yoshinaga, N.; Sano, M. Active motion of a Janus particle by self-thermophoresis in a defocused laser beam. *Physical review letters* **2010**, *105*, 268302.
- (84) Helden, L.; Eichhorn, R.; Bechinger, C. Direct measurement of thermophoretic forces. *Soft matter* **2015**, *11*, 2379–2386.

- (85) Würger, A. Thermophoresis in colloidal suspensions driven by Marangoni forces. *Physical review letters* **2007**, *98*, 138301.
- (86) Liu, Q.; Prosperetti, A. Wall effects on a rotating sphere. *Journal of fluid mechanics* **2010**, *657*, 1–21.
- (87) Fily, Y.; Baskaran, A.; Marchetti, M. C. Cooperative self-propulsion of active and passive rotors. *Soft Matter* **2012**, *8*, 3002–3009.
- (88) Brenner, H. The slow motion of a sphere through a viscous fluid towards a plane surface. *Chemical engineering science* **1961**, *16*, 242–251.
- (89) Jones, P. H.; Maragò, O. M.; Volpe, G. *Optical tweezers: Principles and applications*; Cambridge University Press, 2015.
- (90) Higurashi, E.; Ukita, H.; Tanaka, H.; Ohguchi, O. Optically induced rotation of anisotropic micro-objects fabricated by surface micromachining. *Applied Physics Letters* **1994**, *64*, 2209–2210.
- (91) Galajda, P.; Ormos, P. Complex micromachines produced and driven by light. *Applied Physics Letters* **2001**, *78*, 249–251.
- (92) Wittmeier, A.; Leeth Holterhoff, A.; Johnson, J.; Gibbs, J. G. Rotational analysis of spherical, optically anisotropic janus particles by dynamic microscopy. *Langmuir* **2015**, *31*, 10402–10410.
- (93) Wang, J.; Xiong, Z.; Zhan, X.; Dai, B.; Zheng, J.; Liu, J.; Tang, J. A Silicon nanowire as a spectrally tunable light-driven nanomotor. *Advanced Materials* **2017**, *29*, 1701451.
- (94) Czirók, A.; Ben-Jacob, E.; Cohen, I.; Vicsek, T. Formation of complex bacterial colonies via self-generated vortices. *Physical Review E* **1996**, *54*, 1791.

- (95) Dombrowski, C.; Cisneros, L.; Chatkaew, S.; Goldstein, R. E.; Kessler, J. O. Self-concentration and large-scale coherence in bacterial dynamics. *Physical review letters* **2004**, *93*, 098103.
- (96) Wioland, H.; Woodhouse, F. G.; Dunkel, J.; Kessler, J. O.; Goldstein, R. E. Confinement stabilizes a bacterial suspension into a spiral vortex. *Physical review letters* **2013**, *110*, 268102.
- (97) Riedel, I. H.; Kruse, K.; Howard, J. A self-organized vortex array of hydrodynamically entrained sperm cells. *Science* **2005**, *309*, 300–303.
- (98) Yang, Y.; Elgeti, J.; Gompper, G. Cooperation of sperm in two dimensions: synchronization, attraction, and aggregation through hydrodynamic interactions. *Physical review E* **2008**, *78*, 061903.
- (99) Gadêlha, H.; Hernández-Herrera, P.; Montoya, F.; Darszon, A.; Corkidi, G. Human sperm uses asymmetric and anisotropic flagellar controls to regulate swimming symmetry and cell steering. *Science advances* **2020**, *6*, eaba5168.